Journals
The Institution of Engineering and Technology

An effective time-domain approach for the assessment of the stability characteristics and other nonlinear effects of RF and microwave circuits

ISSN 1751-8644
doi: 0000000000
www.ietdl.org

L. Pantoli[1*], *D. Spina*[2], *D. Romano*[3], *G. Antonini*[3], *G. Leuzzi*[1], *T. Dhaene*[2]

[1] *Department of Industrial and Information Engineering and Economics, University of L'Aquila, Monteluco di Roio, 67100, L'Aquila, Italy*
[2] *IDLab, Department of Information Technology, Ghent University - imec, Technologiepark-Zwijnaarde 15, B-9052 Ghent, Belgium*
[3] *UAq EMC Laboratory, Dipartimento di Ingegneria Industriale e dell'Informazione e di Economia, Università degli Studi dell'Aquila, Via G. Gronchi 18, 67100, L'Aquila, Italy*
* *E-mail: leonardo.pantoli@univaq.it*

Abstract: This paper describes a systematic approach for the stability analysis of RF and microwave nonlinear circuits in the time-domain and that can be useful also for the verification of other nonlinearities, like intermodulation. Time-domain analysis is the most reliable approach for the evaluation of complex nonlinear phenomena but, in general, the transient behaviour of nonlinear circuits is difficult to verify at high frequencies, where distributed elements are common. The solution here addressed overcomes this limitation and it may be applied, without restrictions, also to monolithic microwave integrated circuits and EM-based designs. Examples of application to hybrid prototypes are provided, and the comparison between simulations and measurements illustrates the accuracy and reliability of the proposed approach.

1 Introduction

Stability analysis of RF and microwave nonlinear circuits operating in large-signal regime is crucial for the designers and a challenging task [1]. Because of the complexity of the system evolution when the circuit is driven into nonlinear regime, nonlinearities may arise affecting the circuit behaviour and these issues are even more evident at high frequency. In general, stability issues, like other nonlinear phenomena, are difficult to predict at simulation level due to the characteristics and intrinsic limits of commercial CAD software. In fact, while at low frequencies, a time-domain simulation approach is quite effective and general, at high frequencies time-domain approaches usually experience convergence difficulties or numerical problems, due to the presence of distributed elements and to the high harmonic content of the considered signals. As a result, a frequency-domain approach is the typical choice for the analysis of nonlinear circuits at RF and microwave frequencies. Generally, it proves to be a reliable and effective solution, but it has some shortcomings for the assessment of stability conditions. In fact, frequency-domain solvers, e.g. Harmonic Balance (HB), are based on the assumption of periodic or quasi-periodic signals at given frequencies [2], excluding the analysis of transients that may lead, for instance, to the appearance of spurious signals. A key point in this approach is the numerical calculation of the Fourier series expansion of the nonlinear subnetworks, that is done by means of a Discrete Fourier Transform. This becomes critical in the case of multi-tone quasi-periodic excitation, reducing also the numerical accuracy and increasing the computational time of the algorithm. Furthermore, spurious frequencies are not detected by the HB, since they are not included in the Fourier series expansion.

In order to solve this issue some dedicated approaches for the stability analysis in the frequency-domain have been already proposed in the literature: for example based on the use of an Auxiliary Generator (AG) [1, 3], on pole/zero analysis [4] or on the conversion matrix calculation [5–7]. However, all of them require some compromise: in case of the AG technique [3], for instance, it is assumed that a spurious signal is present and that a rough estimation of its frequency is already available. In particular, the validity of the approach [4] is limited by the reliability of the identification of the rational function in the frequency domain and its extrapolation to the Laplace domain; while, the technique [6, 7] requires a dense discretization of the frequency-domain transfer function in order to evaluate the instability and verify the oscillation.

Also an extension of the HB approach to special cases of transient regime is available [8]. It is based on the assumption that a quasi-periodic signal is modulated by a slowly-changing envelope. In practice, it is addressed to the analysis of narrowband modulation of high-frequency carrier signals, and its accuracy becomes quickly questionable in the case of general signals. Its application to the analysis of spurious signals due to large-signal instability has the same limitations of the AG, and is not suitable to many practical cases.

In the following, we propose an effective and reliable time-domain method for the stability analysis of RF and microwave nonlinear circuits based on the Vector Fitting (VF) algorithm [9, 10]. Such algorithm has been extensively adopted in an electromagnetic compatibility and signal integrity framework, in order to characterize the behavior of distributed elements even in presence of complex nonlinear terminations [11, 12] and only few applications have been already proposed in microwave electronics, limited at system level, as in [13, 14]. The main advantage of the proposed method is its capability to analyze directly in the time-domain any RF and microwave circuit, allowing one to obtain an exhaustive description of the behaviour of the circuits, as typical of low frequency analysis. Hence, a complete and accurate nonlinear stability analysis can be carried out, overcoming the limits of frequency domain-based approaches operating at steady-state [3, 4, 6, 7]. At first, the circuit under study is divided in a linear and passive part (including any distributed or lumped elements) and a nonlinear one (formed by the active elements). Next, the scattering parameters of the linear and passive network are computed over a discrete set of frequencies over the band of interest and a suitable model in a poles-residues form in the Laplace-domain is obtained by means of the Vector Fitting (VF) algorithm [9]. Such model can then be converted in a corresponding equivalent circuit, typically composed of lumped elements and controlled sources [15]. Finally, the lumped elements-based description of the linear and passive network obtained so far can be used in any

Computer-Aided Design (CAD) solver to analyze the performance of the circuit under study. Note that, the proposed approach starts from frequency-domain information (scattering parameters) to compute the desired equivalent circuit, since the properties of passive linear devices are usually only well known in the frequency domain, whether they have been simulated or extracted from measurement.

It is also important to remark that the proposed contribution does not focus on the development of the well-know VF algorithm nor on its synthesis into an equivalent circuit: the aim of the proposed contribution is to define a VF-based analysis methodology for microwave circuits, which is able to describe also the transient behaviour of the device under study, making it particularly suitable for different design activities, including nonlinear analysis and stability issues.

This paper is organized as follows. Section 2.1 summarizes the crucial tasks in transient analysis of RF and microwave circuits; Section 2.2 describes the proposed partitioning of microwave circuits, an overview of the VF algorithm is given in Section 2.3, while macromodeling synthesis techniques are presented in Section 3. The validation of the proposed method is performed in Section 4 by means of four pertinent numerical examples in which both simulations and measurements are provided. Conclusions are summed up in Section 5.

2 Macromodeling

2.1 *Critical tasks in transient analysis*

Time-domain approaches [16], [17] are based on the discretisation in time of the differential equations governing the circuit (Kirkhhof equations), written in terms of voltages and currents, or equivalent quantities. The discretised equations are then numerically solved step by step, yielding voltage and/or currents at all nodes/meshes. This approach is quite effective and general, allowing the simulation of general time-domain waveforms, including transients, for circuits including general nonlinearities. For RF circuits, however, there is a major drawback, that is due to the presence of distributed elements. Their electromagnetic modeling as it is performed by commercial software along with the nonlinear parts results in a large number of differential equations in the time domain which are typically very time consuming to be solved and often fails to converge. In some cases, simple lumped-elements equivalent circuits can be defined for some distributed elements, like transmission lines, but the analysis is accurate only in limited cases. Therefore this approach exhibits severe limitations in most cases.

A mixed approach has been also proposed in the literature and it combines the time-domain analysis of the general network, with a frequency-domain analysis of a linear sub-network [18]. This is not a limitation, since the nonlinear part of an RF circuit can most often be represented by a nonlinear lumped sub-network. The connection between the frequency-domain representation of the distributed linear sub-network and the time-domain algorithm is done via a discrete convolution. While a brilliant solution from a theoretical point of view, the implementation difficulties of the algorithm limit its applicability.

In order to overcome these limitations, we propose a modeling approach that computes an equivalent circuit of the linear and passive elements of RF circuits, which can readily be used for time-domain simulations. Differently from simple equivalent circuits which can be derived from analytical models, the proposed macromodeling approach fully describe the complex behavior of the distributed elements, since it is computed starting from their scattering parameters.

2.2 *Microwave circuit partitioning*

Consider a general microwave network which is in general constituted by an arbitrary number of nonlinear components and linear interconnects. This last part can be efficiently represented resorting to electromagnetic-based modeling techniques, either transmission line models or full-wave techniques. Assuming that the electromagnetic coupling between the distributed linear part and nonlinear devices is quite small and, thus, negligible, an option would be to evaluate separately the model of the interconnect which is physically linear and passive and plug it into the models of the nonlinear devices. Indeed, it is preferable to first compress the model of the passive linear part, since we are only interested to correctly reproduce port voltages and currents. This task can be addressed by using both model-driven or data-driven techniques. To the first family belong model order reduction (MOR) methods [19–21], which use the model equations to generate an approximated model which preserves accuracy and physical properties at the ports. To the second group of reduction techniques belong the methods which only use tabulated data, typically frequency samples of the system response obtained by simulations or measurements, to build a macromodel which still preserves the accuracy and physical properties of the port quantities.

Hence, in order to exploit the possibility to first reduce the linear part of the global microwave circuits, the first step of the proposed methodology relies on the partitioning of the microwave circuit into the passive and active parts, as sketched in Fig. 1. Since the nonlinear part is typically represented in terms of an equivalent circuit, it is useful to retain a circuit model also of the linear part, thus allowing them be connected through n ports characterized by voltages and currents.

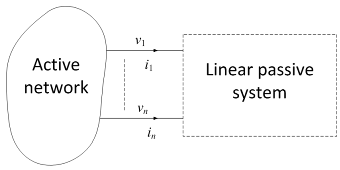

Fig. 1: Partitioning of microwave circuits into nonlinear network and linear passive part.

2.3 *Fitting of S-parameters data*

The proposed method starts with the extraction of the electrical properties of the n-port to be modeled in terms of S-parameters.

$$\mathbf{S}\left(\omega_i\right) = \begin{bmatrix} S_{11}\left(\omega_i\right) & \cdots & S_{1n}\left(\omega_i\right) \\ \vdots & \ddots & \vdots \\ S_{n1}\left(\omega_i\right) & \cdots & S_{nn}\left(\omega_i\right) \end{bmatrix} \tag{1}$$

Typically, the frequency-dependent port parameters $S_{mn}(\omega_i)$ of this matrix will be provided at a set of discrete frequency points $\omega_i = 2\pi f_i, i = 1, \cdots, N_f$, that covers the bandwidth of interest with N_f representing the number of frequency samples. The complex matrix values $S_{mn}(\omega_i)$ in (1) may be obtained either from computer simulations using full-wave electromagnetic field solvers or from measurements with a network analyzer. Our target is to generate a time-domain model of the passive part to be connected to the nonlinear part through suitable port quantities, typically voltages and currents. One possibility is to compute the transient impulse response (impedance or admittance) of the passive part which is to be convolved with the port quantities (currents or voltages). In this case, the samples of the response in the frequency domain are used to generate the impulse response through an inverse Fourier transform (IFT). Typically, a very fine sampling over a wide bandwidth is required to guarantee an accurate transient impulse response. A different methodology is based on the identification of the singularities of the linear system in the complex plane. Indeed, it is known that, from the Jordan's Lemma, a time-domain function $f(t)$ can be

IET Research Journals, pp. 1–11

expressed as [22]

$$
\begin{aligned}
f\left(t\right) &= \frac{1}{2\pi j}\int_{s=\sigma-j\infty}^{s=\sigma+j\infty} F(s)e^{st}ds \\
&= \sum_{all\ poles\ of\ F(s)} Res(F(s))e^{st}
\end{aligned}
\tag{2}
$$

This means that the identification of the singularities of $F(s)$ is sufficient to restore the function $f(t)$.

Hence, the aim of the rational macromodeling is to find a Laplace-domain model (1) in a pole-zero or pole-residue form starting from the knowledge of the frequency response in the frequency-domain. The latter one admits a direct time-domain representation in terms of ordinary differential equations and, thus, it is the most popular. It reads:

$$
\mathbf{S}\left(s\right) = \mathbf{R}_0 + \sum_{k=1}^{n_p} \frac{\mathbf{R}_k}{s-p_k} \tag{3}
$$

where $\mathbf{R}_0 \in \mathbb{R}^{nxn}, \mathbf{R}_k \in \mathbb{C}^{nxn}, k = 1, \cdots, n_p,\ \ n_p$ being the number of poles used to approximate the frequency tabulated data. Typically, all matrix elements $S_{ij}(s)$ of the transfer-matrix representation (3) use a common denominator polynomial and pole-set $\left[p_1, p_2, \cdots, p_{n_p}\right]$, respectively. The identification of poles p_k and residue matrices $\mathbf{R}_k$ can be addressed using several complex curve fitting techniques. The most popular and adopted in this work is the VF algorithm [9]. Note that, fundamental properties for time-domain simulations such as the stability and passivity of models in the form (3) must be assured [11, 14]. While the stability of VF models can be guaranteed by construction by means of suitable pole flipping schemes [9], their passivity can be checked and, eventually, enforced only after the rational model is computed by adopting suitable passivity enforcement techniques. Indeed, due to the unavoidable numerical approximations, the rational model computed might be non-passive. Several robust passivity enforcement methods have been proposed in the literature, see for example [23–26]. The same methodology applies to impedance Z- and admittance Y-based linear models. In the proposed contribution, we have adopted the technique [24] for admittance-based linear sub-systems and the method [25] when fitting scattering parameters responses.

Note that, it is not possible to give here a detailed discussion on rational macromodeling and its passivity enforcement, given the extensive literature on such topics: the interested reader can refer to [9, 11, 23–26] and their references for a complete overview on these subjects. However, some important features of passivity enforcement of rational models will be discussed in the following, given its relevance in the framework of the proposed methodology.

When fitting complex frequency–domain responses over a wide frequency bandwidth, it is possible that the corresponding model in the form (3) will have a high number of poles. In this case, the passivity enforcement phase (if needed) can be expensive, especially for systems with a high number of ports. Furthermore, if the rational model computed exhibits severe passivity violations, its accuracy can be reduced after a passivity enforcement phase. If the accuracy loss is severe, it is preferable to compute a new rational model using different fitting options. Hence, finding an effective rational approximation by means of the VF algorithm when fitting complicated frequency–domain responses over a wide frequency bandwidth can require a good deal of judgment [14].

It is to be pointed out that the macromodeling approach leading to a state-space model is more general than the convolution approach, because it is completely independent on the frequency sampling, meaning that any type of transient solver with fixed or adaptive time stepping can be adopted. Furthermore, the macromodeling approach is well suited to be parameterized. In the last ten years several techniques have been proposed to generate effective parameterized models [27–31].

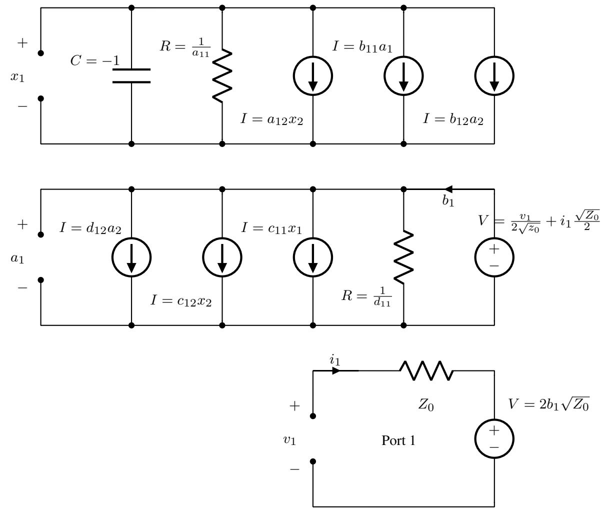

(a) Port 1.

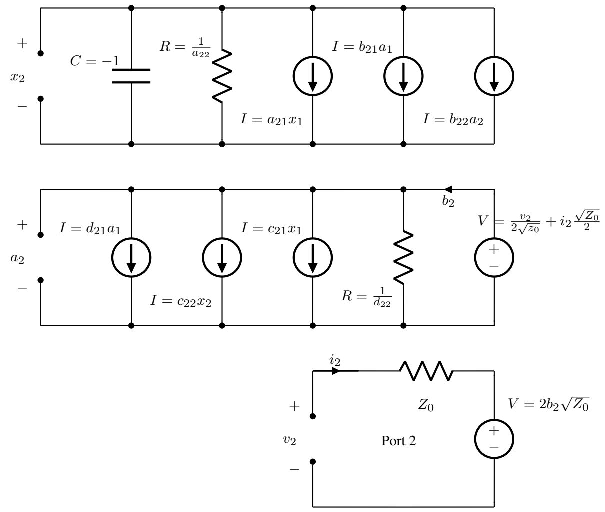

(b) Port 2.

Fig. 2: Illustration of equivalent SPICE network generation from macromodel of a two-port S-parameter data. The incident and reflected waves are indicated by a_k and b_k for $k = 1, 2$, respectively, while the symbols $\left[a_{ij}, b_{ij}, c_{ij}, d_{ij}\right]$ for $i, j = 1, 2$ and and x_k for $k = 1, 2$ represent the elements of the state-space matrices and state-vector in (4), respectively. Note that the unit measure of the circuit element is not indicated in the figure.

3 Synthesis Methods

The derivation of differential equations from a transfer-function system is referred to as macromodeling. In general, a set of first-order differential equations in a state-space form can be described as

$$
\begin{aligned}
\frac{d}{dt}\mathbf{x}\left(t\right) &= \mathbf{A}\mathbf{x}(t) + \mathbf{B}\mathbf{u}(t) \\
\mathbf{y}(t) &= \mathbf{C}\mathbf{x}(t) + \mathbf{D}\mathbf{u}(t)
\end{aligned}
\tag{4}
$$

where $\mathbf{A} \in \mathbb{R}^{mxm}$, $\mathbf{B} \in \mathbb{R}^{mxn}$, $\mathbf{C} \in \mathbb{R}^{nxm}$, $\mathbf{D} \in \mathbb{R}^{nxn}$ and m is the order of the model which equals the number of states. Now, following the approach described in [9], it is possible to compute an equivalent stable and passive state-space representation (4) starting from a model in the form (3), which is suitable for time-domain simulations. Hence, the obtained state-space representation (4) is valid for any general linear and passive network analyzed via the proposed approach. However, simulators such as SPICE do not directly accept differential equations as input. In that case, the macromodel representation given by (4) needs to be converted to an equivalent

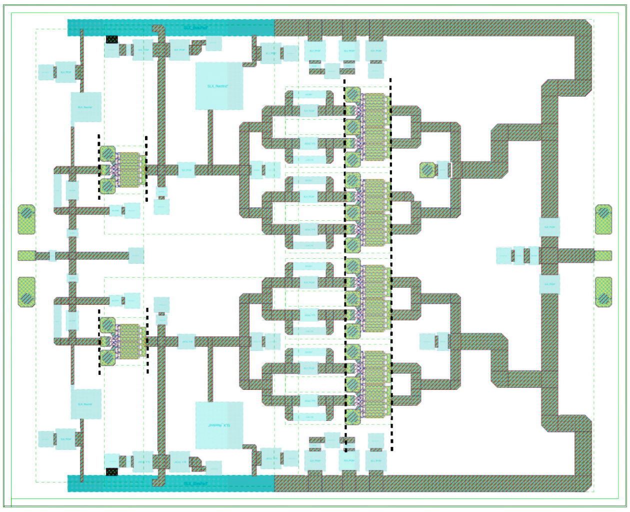

Fig. 3: mPA. Complete layout.

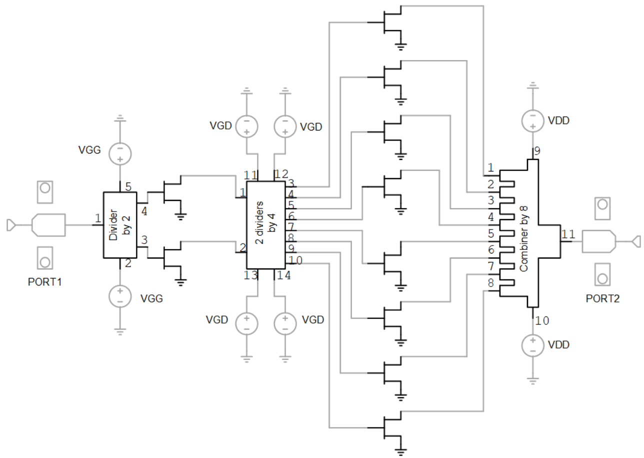

Fig. 4: mPA. Equivalent schematic realized by combining the active devices with the equivalent netlists.

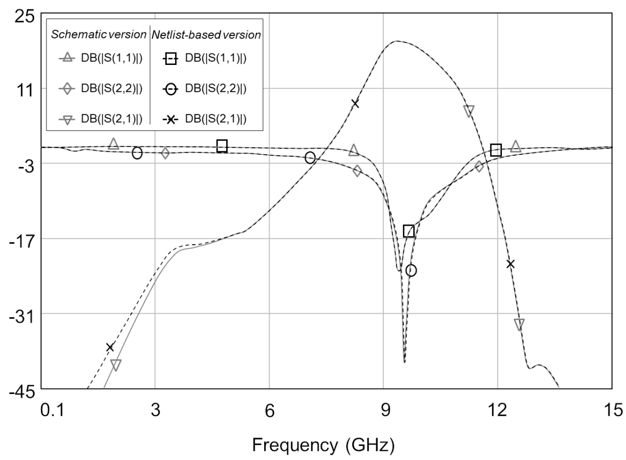

Fig. 5: mPA. Comparison between the S-Parameters obtained with both the schematic version and the netlist-based derived equivalent circuit.

circuit as shown in Fig. 2, via any of the techniques presented in the literature, such as [15, 32–35].

Given the extensive literature on this subject, it is not possible to give here a a detailed description of the different approaches for macromodeling synthesis. However, in order to demonstrate the flexibility of the proposed approach, two different synthesis techniques and simulation environments have been used in the numerical examples in Section 4: an approach based on controlled sources [15] (see Fig. 2) has been used for the second and third test cases presented, analyzed by means of ADS*, while in the first and last numerical examples, studied by means of Microwave Office AWR†, a technique based only on lumped RLC elements has been adopted [34].

4 Analysis of nonlinear effects of RF and microwave circuits

We illustrate the proposed analysis method with four examples of applications on hybrid circuits. The first one provides a feasible demonstration of the robustness of the proposed method in computing accurate equivalent circuit representations, even in case of complex networks; the second and third examples deal with stability analysis; while the forth one is an example addressing intermodulation analysis, so demonstrating the capability of the proposed approach to correctly identify and describe not only stability issues but, more generally, any nonlinear effect. More in detail the first example concerns a two-stage power amplifier operating at 9 GHz with a wide bandwidth; the second one deals with a single-transistor medium power level amplifier; the third example shows the analysis of a passive circuit realizing a frequency division by two, while the fourth one concerns a hybrid medium-power amplifier. It is also important to notice that the prevalent choice of hybrid circuits is not due to any limitation to the application of this approach to integrated circuits. On the contrary, its extension and application to IC solutions is straightforward and even more powerful, considering for example the numerical modelling of complex circuits realized by means of electromagnetic analysis, that includes also layout coupling effects due to layout components close to each others that mutually interact at high frequency for EM radiation effects.

4.1 Modelling of a Multi-Device Parallel Power Amplifier (mPA)

A two-stage multi-device parallel power amplifier realized in GaAs pHEMT technology is considered. It has a first divider-by-2 network, then two driver transistors followed by two additional divider-by-4 networks connected to eight parallel power transistors. Finally a combiner-by-8 passive network finalized by an RF output pad (Fig. 3). The mPA provides 34 dBm output power at 1-dB gain compression point and a linear gain of 16 dB. The circuit experiments some stability concerns in nonlinear regime and has been deeply analyzed in [6], [7]. Unfortunately, the active devices of the available process design kit provided by Selex Foundry cannot be simulated in the time-domain, so transient analysis can not be performed, but the example is quite effective to demonstrate the effectiveness of the proposed synthesis method also in case of large and complex networks and wideband circuits operating in nonlinear regime. The input network (i.e. the divider-by-2 network) is a 5-port network, the interstage (realized by two divider-by-4 networks) is a 14-port network, while the output network (the combiner-by-8 network) is a 11-port network. All of them are analyzed in a wide bandwidth, spanning from 10 MHz until 30 GHz. The partial admittance synthesis approach presented in [34] has been adopted in this example, using 19 poles for the input network, 33 and 43 poles for the interstage and output networks, respectively.

Hence, the mPA can be represented with the novel equivalent circuit in Fig. 4, obtained by suitably connecting the active devices with

*Advanced Design System (ADS), Keysight Technologies, Santa Rosa, CA.
†National Instruments Corporation, Austin, TX

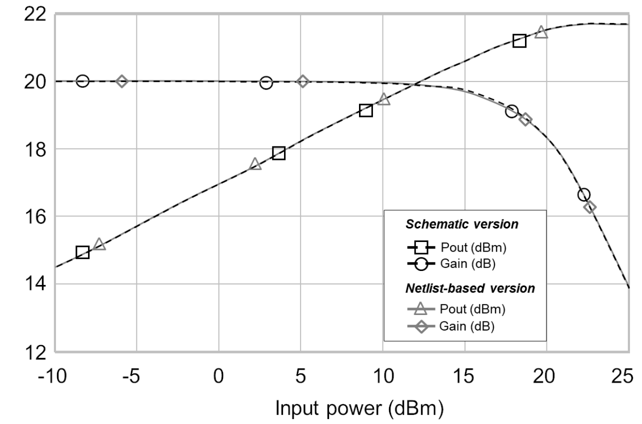

Fig. 6: mPA. Comparison between the nonlinear characteristics of the considered amplifier.

the equivalent netlists obtained for the input, interstage and output network. Figure 5 illustrates an example of the S-parameters of the complete mPA simulated with the original schematic and with the obtained equivalent circuits. The two approaches show a good agreement in a wide frequency bandwidth. Finally, a comparison between the output power and gain obtained with both the schematic version and the netlist-based derived equivalent circuit is reported in Fig. 6, showing a perfect agreement.

4.2 Design of a Spurious-Free Power Amplifier (PA)

The proposed analysis method has been applied to an hybrid medium power level amplifier (MLA) that shows instability problems. The circuit has been designed with the transistor BFR92A, a medium-power BJT from Infineon, modelled with a Gummel-Poon nonlinear model, and fabricated on a TLX8 substrate provided by Taconic. The simplified schematic of the circuit, without distributed components, is shown in Fig. 7. The transistor is biased at $V_{ds} = 7.5$ V with a quiescent collector current of $I_{c0} = 13$ mA. The amplifier has a linear gain of about 16 dB at the considered frequency of 560 MHz, and good input and output match at the same frequency. The MLA, whose prototype is shown in Fig. 8, had been simulated with a standard HB simulator at design stage and tested both in linear and nonlinear regime. Subsequent measurements have shown a parametric subharmonic component with a frequency division by two (Fig. 9), appearing for an input power level greater than about 2 dBm (Fig. 10). So the circuit has revealed a typical nonlinear stability problem, that is difficult to predict by means of commercial CAD software or frequency-domain approaches [3, 4, 6, 7]. Therefore, the circuit has been analyzed by applying the proposed method. The scattering parameters of both the impedance matching and bias networks have been extracted by means of ADS Keysight software, spanning from DC up to the fifth harmonic of the frequency of the input signal. Next, a stable and passive rational model has been computed via the VF algorithm for a 6x6 port model, targeting a maximum absolute error of -45 dB between the scattering parameters and the model response. It required 32 poles. Finally, an equivalent circuit has been computed via both the synthesis method described in Fig. 2 of Section 3 and the one using only RLC elements for the S-parameter representation. They have been used to study the MLA response directly in the time-domain. Figures 11-12 present the time-domain output voltage of the amplifier until steady-state is reached, when a single tone with a power level of 5 dBm is applied at the input port. The simulated traces clearly shows the transient behaviour (Fig. 11) and steady-state behaviour (Fig. 12) of a multi-tone output signal and a signal modulation, revealing the presence of a bifurcation phenomenon in agreement with measurement results.

Note that the simulated oscillation start-up, revealed by the proposed method, is further demonstrated, apart from measurements, with Envelope (EV) simulations on the original circuit. The evolution of both the fundamental and the subharmonic frequency components computed via the native EV solver are superimposed in Fig. 12 on the time-domain signal obtained with the transient analysis in the proposed approach. The amplitude of the spectral components calculated via the EV simulation are coherent with the spectral lines corresponding to the computed time-domain signal. It is important to remark that it has been possible to successfully apply an EV simulation to the original circuits, only by using a time-variant auxiliary generator [3] operating at the bifurcation frequency identified by measurements, necessary to avoid the HB solver convergence to a trivial solution.

A Fast Fourier Transform algorithm, usually already implemented in most CAD tools, can be also applied to the steady-state time-domain simulation data of Fig. 12, and so information concerning both the amplitude and frequency of each spectrum component can be easily computed and verified already at simulation level. In addition, the parametric characteristic and the locus of the bifurcation can be verified by applying the time-domain analysis for several input power levels (Fig. 13). In this way the locus in Fig. 10 obtained by measurements has been found also at simulation level with very good accuracy.

Furthermore, Fig. 14 shows the true, transient evolution of the relationship between input and output voltages at the transistor terminals of the MLA, comparing it with the equivalent trace be obtained via HB simulation on the original circuit. From a theoretical point of view, the number of closed shapes in such curve identifies the number of frequency tones that appear at the output port of the transistor and, consequently, of the amplifier. Figure 14 clearly reveals the dynamic of the system in the transient, since a frequency division by two appears after few nanoseconds and persists at steady-state. It is important to note from the same figure that a traditional HB analysis gives misleading results being unable to detect nonlinear effects at frequencies not included upfront in the simulation setup.

4.3 Characterization of a diode frequency divider (DFD)

This example illustrates the application of the proposed analysis method to the design and characterization of a frequency divider. The time-domain simulation capability allows one to obtain a complete characterization of the proposed circuit; in addition, comparisons with simulations results, obtained with traditional CAD software, demonstrate once again the reliability of this approach to analyze any RF and microwave circuits both in the transient and steady-state domain. In Fig. 15(a), Fig. 15(b) and Fig. 15(c) the considered circuit is shown at both schematic, layout and prototype levels. As shown, the layout is symmetric, but the input and output resonator in the schematic do not make use of the same components. The frequency divider has been designed with a classical design approach, as illustrated in [1] and [36].

It is important to remark that also commercial simulators commonly used for RF and microwave circuits reliably simulate this structure with time-domain solvers, because it has a minimum number of components and compact dimensions with respect to the operational frequency. However, they typically experience convergence or accuracy problems when analyzing more complex structures and circuits with a more distributed nature. Once again, we remark that the proposed simulation method allows to overcome these limitations being a general one, and also providing the possibility to manage the considered circuit both at schematic and at layout (physical) level. Hence, the choice of this circuit is explained to have really a further demonstration of the reliability of the proposed approach by providing a comparison with a native time-domain solver of a CAD software.

The circuit is fabricated on a TLX8 substrate with surface-mount passive components. The diode is a BAS16 from Infineon in an SOT23 package. This frequency divider has been fully characterized in the frequency-domain and measurements are also shown in [1]. In Fig. 15(b) we report the passive section of the circuit that has been modeled with the proposed synthesis method. With respect to the

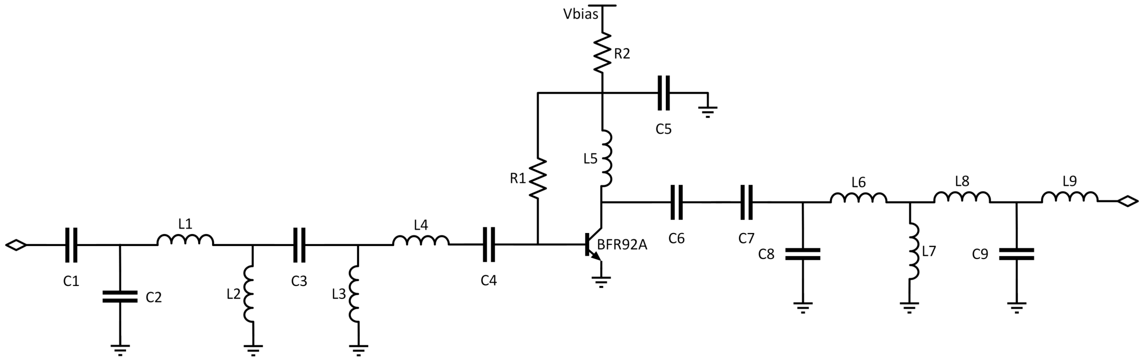

Fig. 7: Simplified schematic of the MLA.

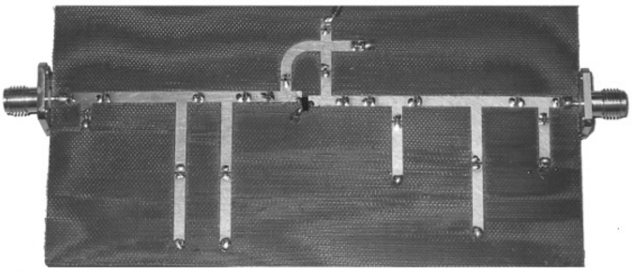

Fig. 8: PA. Photograph of the fabricated amplifier with stability issues.

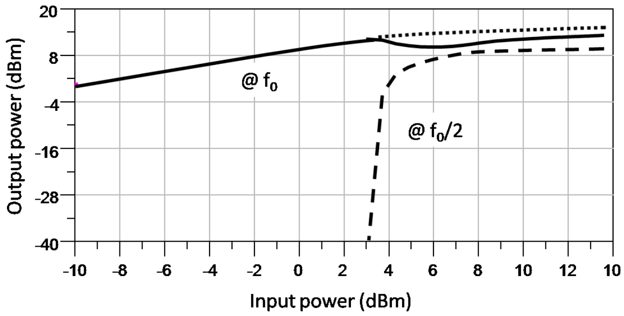

Fig. 10: PA. Measured power transfer function of the unstable amplifier at fundamental frequency (solid line) and sub-harmonic frequency (dashed line). In dotted line the simulated results with a traditional HB simulation.

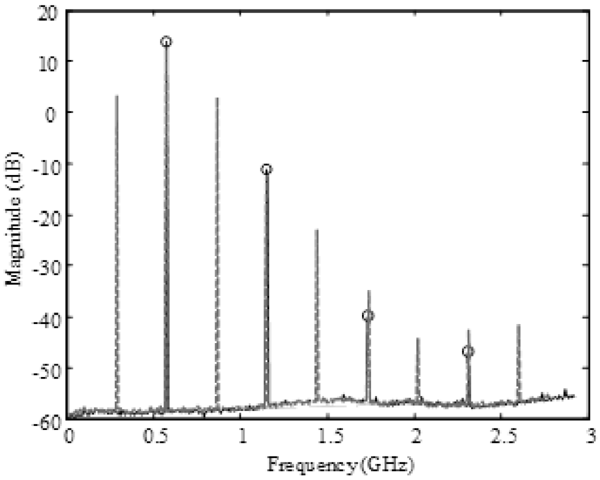

Fig. 9: PA. Output spectrum of the MLA: Measurement results of the reported prototype (dotted grey line) and the simulated one with a standard HB solver (solid line with markers).

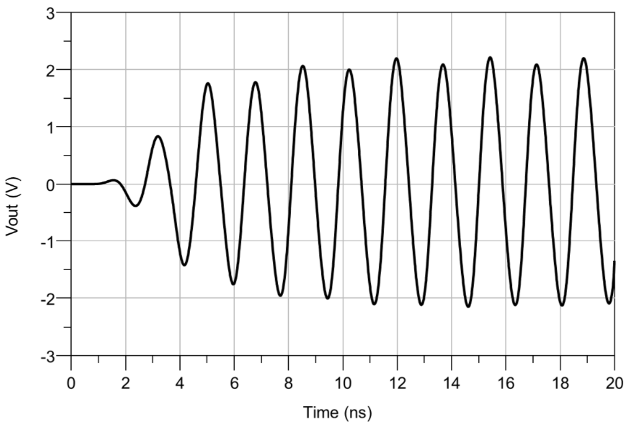

Fig. 11: PA. Initial transient simulation of the output voltage of the unstable amplifier, simulated in the time-domain by turning on a stimulus at 5 dBm of power level and including the proposed equivalent representation of the passive elements of the circuit.

complete circuit (Fig. 15(c)) only the diode has not been included in the modelled network, being it already defined with a nonlinear SPICE model. This section is then analyzed with standard Harmonic Balance solver. EM analysis has not been performed because passive components are defined only by means of S-parameters provided by the manufacturers. The macromodeling of the 3x3 S-parameter matrix of the passive part required 40 poles. The data that have been obtained are then used for the description and simulation in the time-domain of the network in Fig. 15(b). The netlist-based equivalent circuit has been synthesized using the technique described in Fig. 2 and its connection to the lumped elements is reported in the upper left side of Fig. 16. The same figure shows a first comparison between the linear characteristics of the original schematic and those obtained with the derived equivalent model. The S-parameters analysis has been performed up to 2 GHz and results show a perfect agreement.

After the verification of the equivalence of the original network with the modelled one in the frequency-domain, interesting comparisons have been performed in the transient domain, with both envelope transient and time-domain solvers. The frequency divider is designed for an input signal that spans from 600 to 650 MHz; measurements has been performed at 630 MHz with an input power level of 15dBm. In Fig. 17, an Envelope simulation has been performed considering both the native schematic and the netlist-based version of the circuit. Results demonstrate the accuracy of the proposed solution with respect to the original results based on the schematic

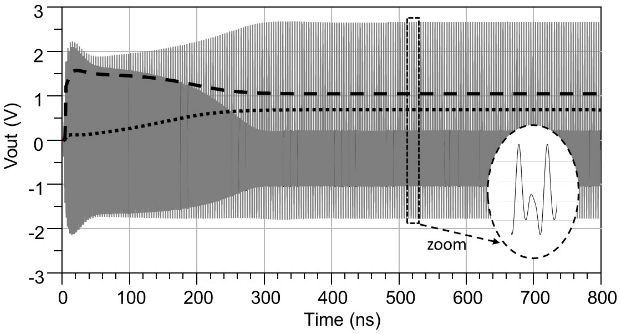

Fig. 12: PA. Transient simulation of the MLA output voltage via the proposed time-domain method (solid grey lines); superimposed, with black lines, the results obtained with EV simulation of the native circuit. In detail, the dashed line represents the time-evolution of the amplitude of the fundamental frequency component, while the dotted line clearly shows the start-up of the sub-harmonic oscillation.

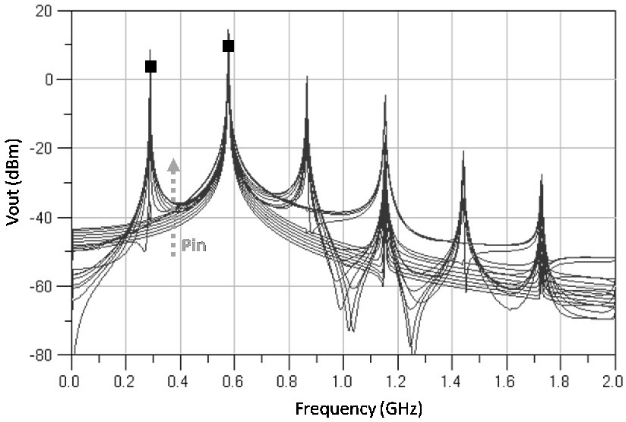

Fig. 13: PA. Output spectrum of the amplifier for different input power levels obtained with a Fast Fourier Transform of the proposed time-domain analysis. The amplitude of the spectral lines obtained via the EV simulation of Fig. 12 is also highlighted with squared markers.

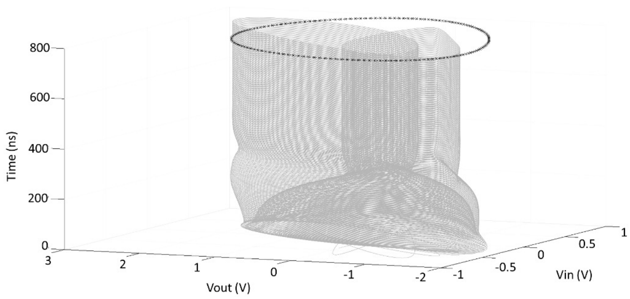

Fig. 14: PA. Transient evolution of the relationship between input and output voltages at the transistor terminals of the MLA obtained via the proposed method for a stimulus at 5 dBm of power level. Superimposed, with a black line, the equivalent relationship obtained at steady-state with an HB simulation.

version of the circuit. Only small differences arise in the initial 10 ns, but they are caused by the poor convergence obtained simulating the native circuit due to the presence of distributed elements and S-parameter-based passive components. Anyway, the capability to detect the sub-harmonic oscillation condition is clearly shown, as discussed in [5]. Finally, the same comparison has been carried out with a time-domain transient simulator, that is the better solver

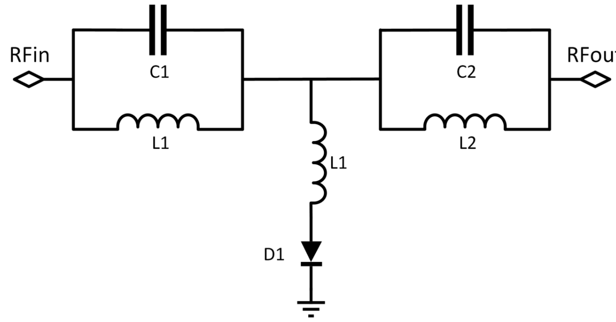

(a)

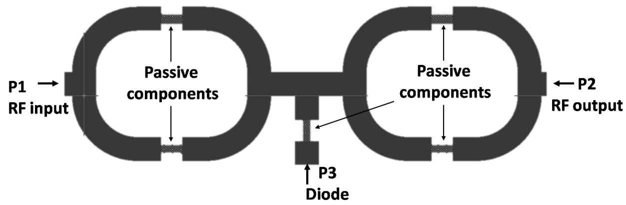

(b)

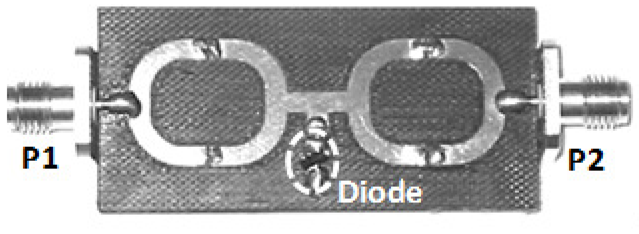

(c)

Fig. 15: DFD. a) Simplified schematic; b) Layout of the passive network considered for the generation of the equivalent SPICE model; c) Fabricated prototype of the frequency divider.

for the analysis of complex nonlinear phenomena or for synchronization of subcircuits. Also in this case, the results are satisfactory. Figures 18(a) and 18(b) show the transient response and the steady-state time-domain results, respectively, when an input signal at 630 MHz with a power level of 15 dBm is applied to the frequency divider. Once again, the small inaccuracies, mainly in the transient, are accountable to the simulation difficulties that arise when considering the original distributed circuit, since in this case convergence can be obtained only by relaxing the convergence error requirements. It is important to remark that usually the transient solver works with difficulty even considering simple circuits like this frequency divider, while cannot be used at all with more complex circuits.

Finally, the Fourier Transform of the time-domain simulation of the netlist-based equivalent circuit is compared in Fig. 19 with the spectrum obtained with and Harmonic Balance simulation of the original circuit. As illustrated, the agreements is very good up to high order harmonics, so confirming the capability to describe the signal in any nonlinear circuit by Fourier and/or Laplace transforms. Results are consistent also with measurements, showing the circuit a parametric frequency division by two for an increasing input power level, as clearly illustrated in [1]. For the sake of illustration, Fig. 20 shows the measured output spectrum considering an input signal with a power level of 18 dBm.

4.4 Intermodulation analysis on a medium-power amplifier (MPA)

This example is a further proof of the accuracy of the proposed time-domain analysis method for the verification of nonlinear effects in

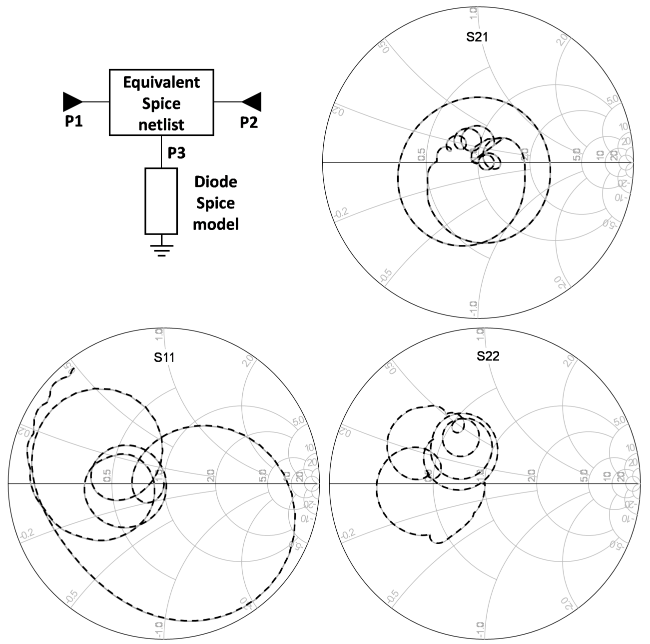

Fig. 16: DFD. Simulated S-parameters of the frequency divider up to 2GHz: comparison between the linear characteristics of the original schematic (black dashed lines) and those of the netlist-based equivalent circuit as defined in the same picture (grey solid lines).

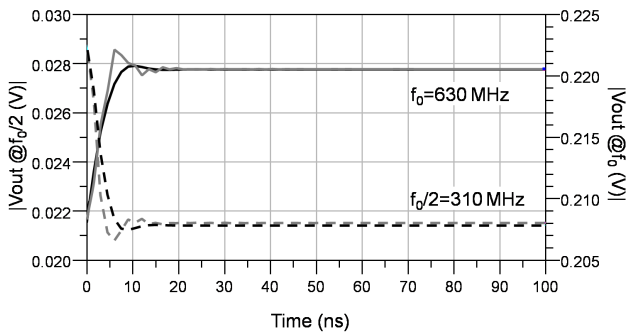

Fig. 17: DFD. Envelope simulations: comparison between the traces obtained with the original schematic (grey lines) and those with the netlist-based equivalent circuit (black lines).

microwave active circuits. The case study proposed here is a simple medium power level amplifier realized with hybrid components and a single bipolar transistor, the BFP450 from Infineon. Figure 21(a) illustrates the simplified schematic of the circuit, while a photograph of the prototype is shown in Fig. 21(b). The amplifier has 12 dB gain at the centre frequency of 1.75 GHz with an output power at 1-dB gain compression point of 15 dBm. The circuit has been simulated and tested with good results both in linear regime (S-parameters analysis) and nonlinear regime (power transfer function and intermodulation analysis).

The nonlinearities of this circuit have been evaluated also with the time-domain analysis method here proposed in order to check the validity of this approach with respect to more complex nonlinear phenomena as, for instance, the evaluation of the third-order intercept point (IP3). With this aim, the passive networks of the amplifier modelled with both lumped and distributed elements have been considered together as part of the passive network shown in Fig. 22. Next, an equivalent 7x7 SPICE network has been computed by means of the proposed method, which can be included in any CAD simulation software as a common 7-ports netlist. In detail, the following ports have been considered: RF input, RF output, base terminal, collector terminal, 2 emitter terminals, DC bias pad, as indicated in Fig. 22 by arrows. In particular, the emitter terminals

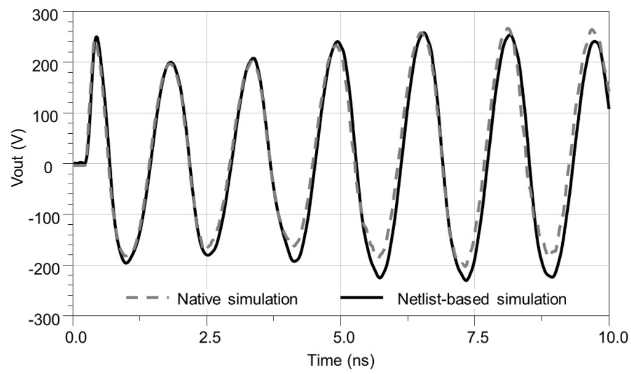

(a)

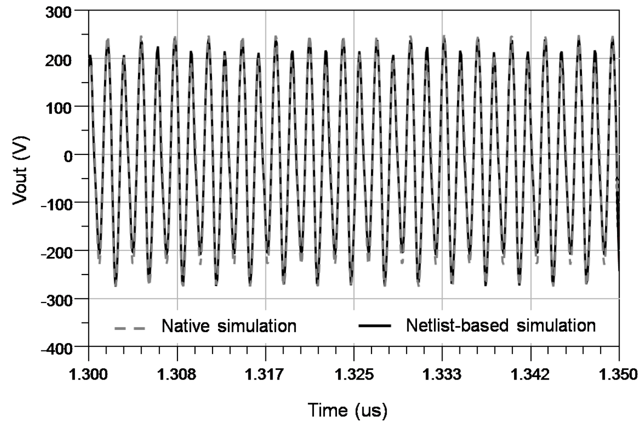

(b)

Fig. 18: DFD. Time-domain simulations. Comparison between the output voltage obtained with the original schematic (grey dotted line) and by means of the netlist-based equivalent circuit (black solid line) in the transient regime (a) and at steady-state (b).

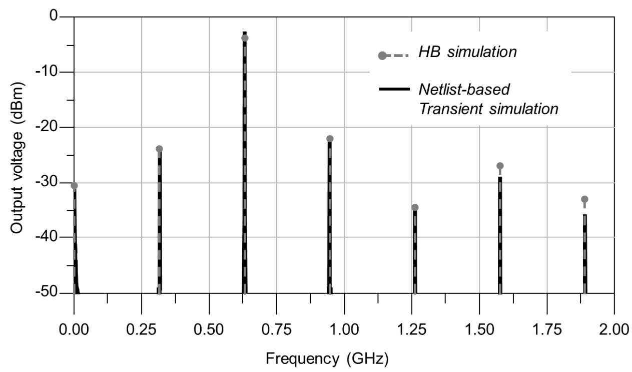

Fig. 19: DFD. Fourier Transform of the time-domain simulation of the output voltage obtained with the netlist-based equivalent circuit (black solid line), compared with the output spectrum obtained with an Harmonic Balance simulation of the original schematic (grey dotted line).

are considered since, in general, the transistor is very sensitive to the emitter load, in particular for what concern stability. In this case, these two ports are useful to model the via holes that directly connect the emitters of the active device to ground. Whereas, the DC bias port is taken into account in order to analyze the circuit also considering the load seen by the amplifier on the bias line. This is possible since the derived equivalent network is defined from DC up to high frequency (in order to include all significant harmonics of the input signal and properly analyze the nonlinearities of the circuit).

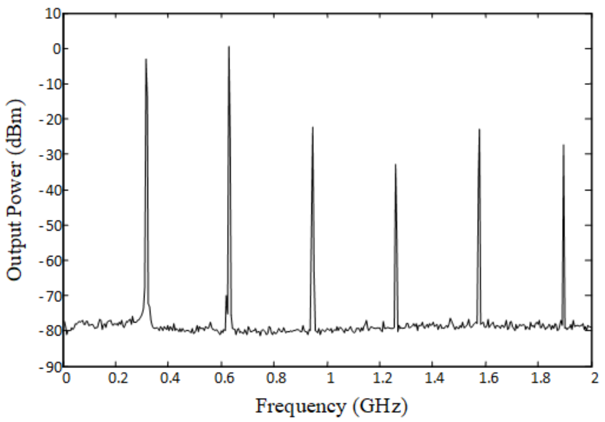

Fig. 20: DFD. Measured output power spectra of the DFD for an input power Pin=18 dBm.

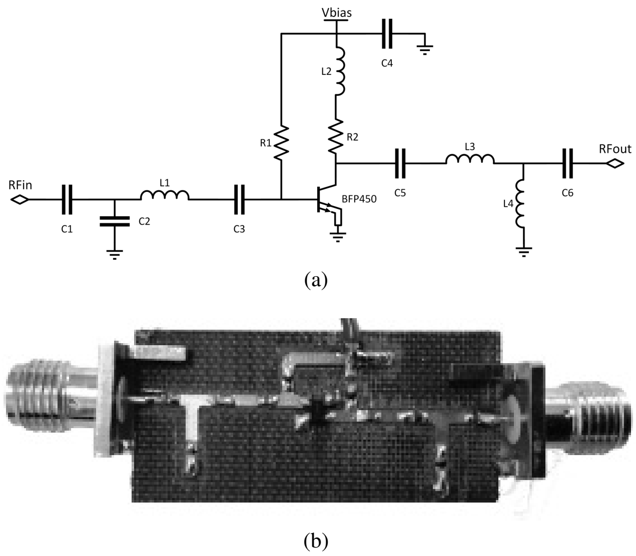

Fig. 21: MPA. (a) Simplified schematic; (b) Prototype of the hybrid, medium-power amplifier.

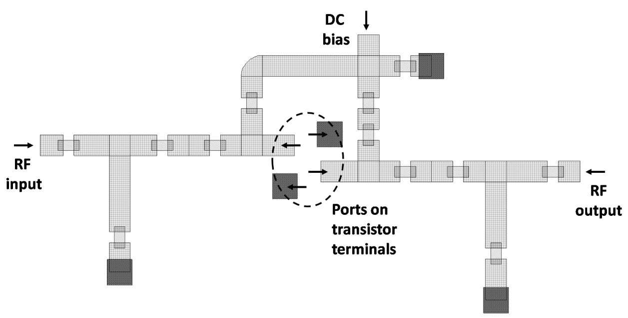

Fig. 22: MPA. Passive network of the amplifier that has been considered for the generation of the time-domain equivalent model.

The partial admittance synthesis approach presented in [34] has been adopted using 45 poles. Once again, it is important to remark that this is an important advantage for the designer since it allows the simulation of any distributed circuit or EM based networks also in the time-domain with good accuracy.

A new schematic is then considered, including the SPICE models of both the active device and the passive circuitry. This system can be obviously simulated with any solvers, as already shown in

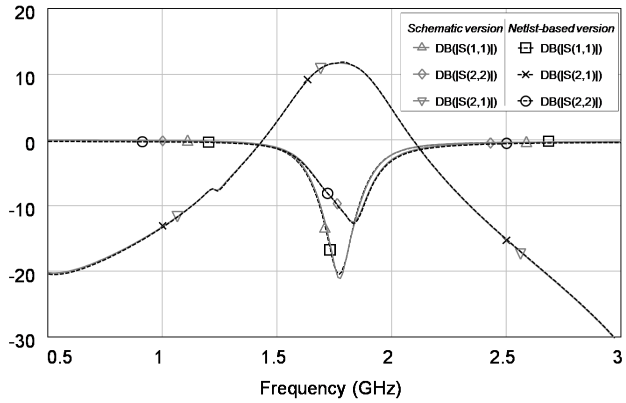

Fig. 23: MPA. Comparison between the S-Parameters obtained with both the schematic version and the netlist-based derived equivalent circuit.

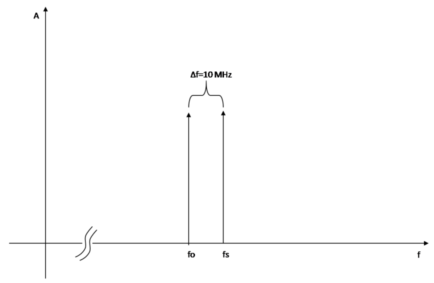

Fig. 24: MPA. Two-tones signal that has been considered for intermodulation analyses.

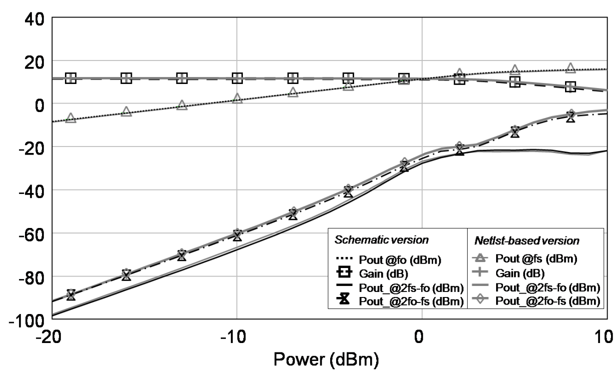

Fig. 25: MPA. Comparison between the nonlinear characteristics of the considered amplifier. Gain, output power and intermodulation levels of both the schematic version and the netlist-based derived equivalent version.

the previous examples. Now some additional results are shown, including higher order nonlinear effects in the frequency-domain. In Fig. 23 simulation results are shown with the S-parameters of the complete amplifier described with the original schematic and with the defined equivalent circuits. The agreement between the two approaches is excellent in the small signal regime. As a final step, also the large signal behaviour has been checked in terms of compression and intermodulation levels. The 1-dB gain compression point analysis has been carried out considering a single tone input signal at 1.75 GHz with a power range from -20 to 10 dBm. The third-order intercept point has been evaluated with a two-tone analysis with an input signal as defined in Fig. 24, where a second tone is present at frequency *fs* spaced 10 MHz away from the fundamental tone *fo* at 1.75 GHz. Final results are shown in Fig. 25, where we report output power and intermodulation characteristics versus input

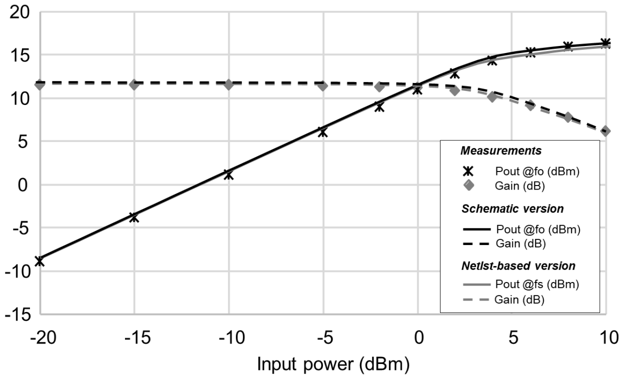

Fig. 26: MPA. Measured gain and output power compared with the equivalent parameters of both the schematic version and the netlist-based derived equivalent version.

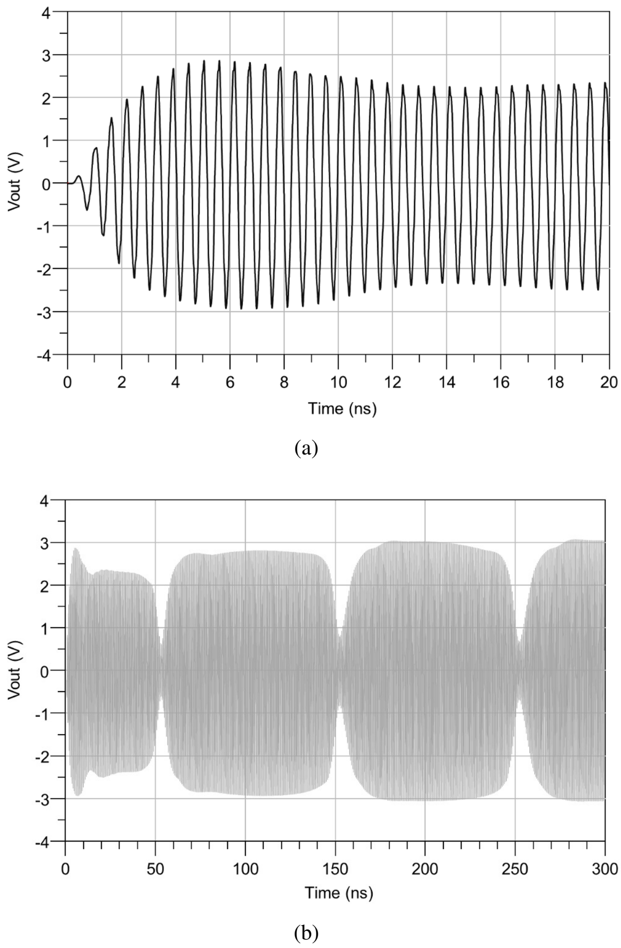

Fig. 27: MPA. Time-domain simulations obtained considering the netlist-based equivalent circuit and the two-tone input signal as defined in Fig. 24. Both the transient response (a) and the steady-state evolution (b) are relative to a stimulus at a power level of 3dBm, that is the 1dB compression point of the considered amplifier, as shown in Fig. 25.

power for both the original schematic version of the amplifier and the netlist-based equivalent description here provided. A feasibility demonstration of the accuracy of the proposed design is provided in Fig. 26, where the measured gain and output power of the hybrid prototype are reported and show a good agreement with simulated results.

As a further proof of concept, the transient analysis has been carried out also on this circuit, once described with the netlist-based equivalent version. The stimulus has been defined as a two-tone signal, as shown in Fig. 24 and applying a power level of 3 dBm, so considering the amplifier working around the 1 dB compression point, when nonlinear effects clearly arise. Figure 27(a) shows the transient response of the amplifier, while Fig. 27(b) depicts the evolution of the output signal in the time-domain and describes the intermodulation phenomena due to the active device nonlinearities and the multi-tone input signal.

5 Conclusions

In this work a systematic approach for the analysis of nonlinear circuits at RF and microwave frequencies in both transient and steady-state regimes has been proposed. The time-domain analysis of a distributed circuits is usually a missing resource for the designer in particular for those circuits which make use of distributed elements, as it usually happens at higher frequencies. By the use of a synthesis approach of the passive networks based on the VF method and circuit synthesis techniques, general nonlinear circuits can be successfully analyzed both in the time- and frequency-domain in a SPICE-like framework. The proposed technique allows one to verify, at simulation level, complex nonlinear behaviours, as for instance the start-up of oscillations, bifurcation phenomena and intermodulation characteristics. Suitable experimental examples have been presented and measurements are also provided confirming the validity of the proposed approach.

L. Pantoli, D. Romano, G. Antonini and G. Leuzzi (*Department of Industrial and Information Engineering and Economics, University of L'Aquila, Monteluco di Roio, L'Aquila, Italy*)

E-mail: leonardo.pantoli@univaq.it

D. Spina and T. Dhaene (*IDLab, Department of Information Technology, Ghent University - imec, Ghent, Belgium*)

6 References

1 Pantoli, L., Suarez, A., Leuzzi, G., Di Paolo, F.: 'Complete and Systematic Simulation Tools for Frequency Divider Design', *IEEE Trans. Microw. Theory Techn.*, 2008, **56**, (11), pp. 2442–2452
2 Kundert, K.S., Sangiovanni-Vincentelli, A.:'Simulation of Nonlinear Circuits in the Frequency Domain', *IEEE Trans. Comput.-Aided Design Integr. Circuits Syst.*, 1986, **5**, (4), pp. 521–535
3 Ramirez, F., de Cos, M.E., Suarez, A.: 'Nonlinear analysis tools for the optimized design of harmonic-injection dividers', *IEEE Trans. Microw. Theory Techn.*, 2003, **51**, (6), pp. 1752–1762
4 Jugo, J., Portilla, J., Anakabe, A., Suarez, A., Collantes, J.M.: 'Closed-loop stability analysis of microwave amplifiers', *Electron. Lett.*, 2001, **37**, (4), pp. 226–228
5 Pantoli, L.: 'Transient-based conversion matrix approach for nonlinear stability analysis', *Electron. Lett.*, 2014, **50**, (13), pp. 923–925
6 Pantoli, L., Leuzzi, G., Santarelli, A., Filicori, F. Giofré, R.: 'Stabilisation approach for multi-device parallel power amplifiers under large-signal regime', *6th European Microwave Integrated Circuit Conference*, 2011, pp. 144–147
7 Pantoli, L., Leuzzi, G., Santarelli, A., Filicori, F.: 'Stability Analysis and Design Criteria of Paralleled-Device Power Amplifiers Under Large-Signal Regime', *IEEE Trans. Microw. Theory Techn.*, 2016, **64**, (5), pp. 1442–1455
8 Ngoya, E., Larcheveque, R.: 'Envelop transient analysis: a new method for the transient and steady state analysis of microwave communication circuits and systems', *IEEE MTT-S International Microwave Symposium Digest*, 1996, **3**, pp. 1365–1368
9 Gustavsen, B., Semlyen, A.: 'Rational approximation of frequency domain responses by Vector Fitting', *IEEE Trans. Power Del.*, 1999, **14**, (3), pp. 1052–1061
10 Deschrijver, D., Mrozowski, M., Dhaene, T., De Zutter, D.: 'Macromodeling of Multiport Systems Using a Fast Implementation of the Vector Fitting Method', *IEEE Microw. Wirel. Compon. Lett.*, 2008, **18**, (6), pp. 383–385
11 Grivet-Talocia, S., Gustavsen, B.: 'Black-box macromodeling and its EMC applications', *IEEE Electromagn. Compat.*, 2016, **5**, (3), pp. 71–78
12 Spina, D., Ferranti, F., Antonini, G., Dhaene, T., Knockaert, L., Vande Ginste, D.: 'Time-Domain Green's Function-Based Parametric Sensitivity Analysis of Multiconductor Transmission Lines', *IEEE Trans. Compon., Packag., Manuf. Technol.*, 2012, **2**, (9), pp. 1510–1517
13 Brazil, T.J.: 'Nonlinear transient simulation of mixed EM/circuit-level system blocks'. Proc. International Conference on Numerical Electromagnetic Modeling and Optimization for RF, Microwave, and Terahertz Applications (NEMO), Pavia, Italy, 2014
14 Brazil, T.J.: 'Time-domain techniques in microwave circuit simulation', *IET Microw. Antenna P.*, 2013, **7**, (2), pp. 146–155

15 Neumayer, R., Haslinger, F., Stelzer, A., Weigel, R.: 'Synthesis of SPICE-compatible broadband electrical models from n-port scattering parameter data'. Proc. IEEE International Symposium on Electromagnetic Compatibility, Minneapolis, USA, 2002, pp. 469–474
16 Nagel, L.W.: 'SPICE2: A Computer Program to Simulate Semiconductor Circuits', Ph.D. dissertation, EECS Department, University of California, Berkeley, 1975. [Online]. Available: http://www2.eecs.berkeley.edu/Pubs/TechRpts/1975/9602.html
17 Vendelin, G.D., Pavio, A.M., Rohde, U.L.: 'Microwave Circuit Design Using Linear and Nonlinear Techniques', Wiley-IEEE Press, 2005
18 Brazil, T.J.: 'Causal-convolution-a new method for the transient analysis of linear systems at microwave frequencies', *IEEE Trans. Microw. Theory Techn.*, 1995, **43**, (2), pp. 315–323
19 Samuel, E.R., Knockaert, L., Dhaene, T.: 'Model Order Reduction of Time-Delay Systems Using a Laguerre Expansion Technique', *IEEE Trans. Circuits Syst. I, Reg. Papers.*, 2014, **61**, (6), pp. 1815–1823
20 Oyaro, D., Triverio, P.: 'TurboMOR-RC: An Efficient Model Order Reduction Technique for RC Networks With Many Ports', *IEEE Trans. Comput.-Aided Design Integr. Circuits Syst.*, 2016, **35**, (10), pp. 1695–1706
21 Zulfiqar, U., Imran, M., Ghafoor, A.: 'Cross-Gramian based frequency-weighted model order reduction technique', *Electron. Lett.*, 2016, **52**, (16), pp. 1376–1377
22 Kreyszig, E.: 'Advanced Engineering Mathematics', Wiley, 2011
23 Grivet-Talocia, S. Ubolli, A.: 'A Comparative Study of Passivity Enforcement Schemes for Linear Lumped Macromodels', *IEEE Trans. Adv. Packaging*, 2008, **31**, (4), pp. 673–683
24 Gustavsen, B.: 'Fast Passivity Enforcement for Pole-Residue Models by Perturbation of Residue Matrix Eigenvalues', *IEEE Trans. Power Del.*, 2008, **23**, (4), pp. 2278–2285
25 Gustavsen, B.: 'Fast Passivity Enforcement for S-Parameter Models by Perturbation of Residue Matrix Eigenvalues', *IEEE Trans. Adv. Packaging*, 2010, **33**, (1), pp. 257–265
26 Deschrijver, D., Dhaene, T.: 'Fast Passivity Enforcement of S-Parameter Macromodels by Pole Perturbation," *IEEE Trans. Microw. Theory Techn.*, 2009, **57**, (3), pp. 620–626
27 Ferranti, F., Antonini, G., Dhaene, T., Knockaert, L., Ruehli, A.E.: 'Physics-Based Passivity-Preserving Parameterized Model Order Reduction for PEEC Circuit Analysis', *IEEE Trans. Compon., Packag., Manuf. Technol.*, 2011, **1**, (3), pp. 399–409
28 Ferranti, F., Nakhla, M., Antonini, G., Dhaene, T., Knockaert, L., Ruehli, A.E.: 'Interpolation-Based Parameterized Model Order Reduction of Delayed Systems', *IEEE Trans. Microw. Theory Techn.*, 2012, **60**, (3), pp. 431–440
29 Samuel, E.R., Ferranti, F., Knockaert, L., Dhaene, T.: 'Passivity-Preserving Parameterized Model Order Reduction Using Singular Values and Matrix Interpolation', *IEEE Trans. Compon., Packag., Manuf. Technol.*, 2013, **3**, (6), pp. 1028–1037
30 Ferranti, F. and Knockaert, L. and Dhaene, T. and Antonini, G.: 'Passivity-Preserving Parametric Macromodeling for Highly Dynamic Tabulated Data Based on Lur'e Equations', *IEEE Transactions on Microwave Theory and Techniques*, 2010, **58**, (12), pp. 3688–3696
31 Passos, F., Ye, Y., Spina, D., Roca, E., Castro-López, R., Dhaene, T., Fernández, F.: 'Parametric macromodeling of integrated inductors for RF circuit design', *Microw. Opt. Technol. Lett.*, 2017, **59**, pp. 1207–1212.
32 Qi, Z., Yu, H., Liu, P., Tan, S.X.D., He, L. :'Wideband passive multiport model order reduction and realization of RLCM circuits', *IEEE Trans. Comput.-Aided Design Integr. Circuits Syst.*, 2006, **25**, (8), pp. 1496–1509
33 Villena, J.F., Silveira, L.M.:'Circuit Synthesis for Guaranteed Positive Sparse Realization of Passive State-Space Models', *IEEE Trans. Circuits Syst. I*, 2017, **64**, (6), pp. 1576–1587
34 Antonini, G.:'SPICE Compatible Equivalent Circuits of Rational Approximation of Frequency Domain Responses', *IEEE Electromagn. Compat.*, 2003, **45**, (3), pp. 502–512
35 Majumdar, P., Zhao, Z., Yue, Y., Ji, C., Liu, R.: 'Equivalent circuit model of cross and circular ring FSS using vector fitting'. Proc. 3rd Asia-Pacific Conference on Antennas and Propagation, Harbin, China, 2014
36 Suarez, A. Melville, R.: 'Simulation-assisted design and analysis of varactor-based frequency multipliers and dividers', *IEEE Trans. Microw. Theory Techn.*, 2006, **54**, (3), pp. 1166–1179